

# Dynamics of simple magnetorheological suspensions under rotating magnetic fields with modulated Mason number

Oscar G Calderón<sup>1,2,3</sup> and Sonia Melle<sup>2</sup>

<sup>1</sup> Dpto. Optica, Universidad Complutense de Madrid, Ciudad Universitaria s/n, Madrid 28040, Spain

<sup>2</sup> Dpto. Física Fundamental, UNED, Paseo Senda del Rey 9, Madrid 28040, Spain

E-mail: oscargc@opt.ucm.es

Received 5 April 2002

Published 8 October 2002

Online at [stacks.iop.org/JPhysD/35/2492](http://stacks.iop.org/JPhysD/35/2492)

## Abstract

We study theoretically the dynamics of a system of two magnetizable particles suspended in a non-magnetic fluid subject to a rotating magnetic field when a modulation on the Mason number (ratio of viscous to magnetic forces) is applied. We find, using a periodic modulation, that a resonant-like phenomenon between the periodic modulation of the Mason number and the intrinsic radial oscillation of the system without modulation occurs. For a random perturbation of the Mason number, we obtain an optimum noise strength at which the average interparticle distance reaches the lowest value. When a weak periodic modulation and a noise source are included in the Mason number, stochastic resonance (SR) is found for different frequencies and amplitudes of the modulation. An interpretation of this SR phenomenon is made by means of a threshold crossing mechanism.

## 1. Introduction

Magnetorheological (MR) suspensions consist of magnetizable particles (diameter  $\sim 1\text{--}10\ \mu\text{m}$ ) suspended in a non-magnetic fluid. They possess the unique ability to undergo rapid (within a few milliseconds), nearly completely reversible, significant changes in their strength (yield stress change from  $\sim 0$  to 100 kPa) upon application of an external magnetic field [1]. This significant change in flow behaviour is accompanied by a change in suspension microstructure. When exposed to an external magnetic field, the particles in a MR suspension acquire dipole moments and, due to the induced dipolar interactions, aggregate to form chain-structures aligned with the field. These structures restrict the motion of the fluid, thereby increasing the viscosity of the suspension (up to  $10^5\text{--}10^6$  times).

Most of the studies to date have focused on the response of MR suspensions to unidirectional magnetic fields [2–6]. However, in the last few years their response to rotating magnetic fields has been a research area of new interest. Thus, Helgesen *et al* [7] carried out experiments on a system of two magnetic holes (non-magnetic microspheres in a ferrofluid)

subject to a rotating magnetic field. They found two different rotating regimes depending on the value of the rotating frequency being below or above a threshold frequency. At low frequencies, the pair rotates uniformly and is phase-locked to the field. However, once the frequency overcomes a threshold value, the pair is not able to follow the field due to the viscous friction so its phase lag increases with time until it reaches the value  $\pi/2$ . Beyond this point, the magnetic torques reverse sign, forcing the pair to rotate backwards. This continues until the field ‘catches up’ with the pair (zero phase lag) and a new cycle of forward and backward rotation takes place. Furthermore, in this asynchronous rotation regime, an additional radial oscillation of the pair is observed in which the particles separate a certain distance each time that the axis between the particles rotates opposite to the field. At the same time, Kashevsky and Novikova [8, 9] theoretically studied the interactions between pairs of magnetic particles or magnetic holes under rotating fields predicting a similar behaviour. In a more recent work Kashevsky and Kuzmin [10] showed that hydrodynamic interaction makes the pair behaviour very sensitive to the particle surface conditions.

The behaviour of a system formed by up to seven particles in a rotating magnetic field were reported by

<sup>3</sup> Author to whom correspondence should be addressed.

Meakin and Skjeltorp [11]. Different rotational modes were found depending on the rotating frequency. At high rotating frequencies these modes became extremely complicated and chaotic states were found. Experimental studies regarding multiparticle dynamics under rotating magnetic fields have been recently reported in MR suspensions using scattering dichroism [12, 13] and microscopy [14]. In these works the formation of chains that rotate with the field but lag behind by a constant phase angle has been shown. We also found that the Mason number,  $Ma$  (ratio of viscous to magnetic forces), governs the dynamics of the field-induced dipolar chains under rotating fields. This dimensionless parameter<sup>4</sup> is given by [15–17]

$$Ma = \frac{12^2 \eta \omega_0}{\mu_s \mu_0 M^2}, \quad (1)$$

where  $\eta$  is the solvent viscosity,  $\omega_0$  is the field rotating frequency, and  $\mu_s$  and  $\mu_0$  are the solvent and vacuum magnetic permeability, respectively. A cross-over Mason number was found above which the viscous forces dominate and inhibit the aggregation process.

In this paper, we theoretically study the dynamics of simple MR suspensions under rotating magnetic fields when a modulation on the Mason number is applied. The system consists of a pair of magnetizable particles immersed in a non-magnetic fluid. We analyse the behaviour of the system for different types of perturbations on  $Ma$ . Using a periodic modulation, we observe that a resonant-like phenomenon between the periodic modulation of  $Ma$  and the intrinsic radial oscillation of the system without modulation occurs. When a weak periodic modulation and a noise source are included in the Mason number, the stochastic resonance (SR)<sup>5</sup> is found for different frequencies and amplitudes of the modulation (see reviews [18]). This phenomenon has been theoretically predicted for ferromagnetic monodomain particles dispersed in a solid phase when an alternating magnetic field is imposed [19]. Recently, Alarcón and Pérez-Madrid have found that a ferromagnetic dipole immersed in a shear flow exhibits SR when a weak oscillating magnetic field is acting on it [20].

## 2. Theoretical model

We consider a pair of spherical magnetizable particles of diameter  $2a$  suspended in a fluid of viscosity  $\eta$  and subject to rotating magnetic fields of amplitude  $H_0$  and angular frequency  $\omega_0$

$$\vec{H} = H_0(\cos(\omega_0 t)\hat{x} + \sin(\omega_0 t)\hat{y}). \quad (2)$$

When the magnetic field is applied the particles acquire a dipole moment  $\vec{m} = (4\pi/3)a^3\vec{M}$ , where  $2a$  is the particle diameter, and  $\vec{M} = \chi\vec{H}$  is the particle magnetization; here  $\chi$  is the particle magnetic susceptibility. We assume that the magnetic interaction of the particles dominates their random thermal motion. In other words, the key dimensionless parameter

<sup>4</sup> Mason number was first introduced in literature for electrorheological fluids under steady shear.

<sup>5</sup> The term SR is given to a phenomenon that is manifest in nonlinear systems whereby generally feeble input information (such as a weak signal) can be amplified and optimized by the assistance of noise.

that measures the ratio of magnetic to thermal energies will be much larger than one,  $\lambda \gg 1$ . This ratio is defined as  $\lambda = \mu_0 \mu_s m^2 / 16\pi a^3 k_B T$ , where  $k_B$  is the Boltzmann constant, and  $T$  is the temperature. Neglecting the inertia term, and considering Stokes friction against the solvent, the equation of motion of the pair is

$$\gamma \frac{d\vec{r}}{dt} = 2\vec{F}^m + 2\vec{F}^{ev}, \quad (3)$$

where  $\gamma = 6\pi\eta a$  is the Stokes drag coefficient,  $\vec{r} \equiv \vec{r}_2 - \vec{r}_1$ ,  $\vec{r}_1$  and  $\vec{r}_2$  being the positions of particles 1 and 2, respectively. We use the point-dipole approximation to compute the magnetic force  $\vec{F}^m$ , i.e.

$$\vec{F}^m = \frac{3\mu_0 m^2}{2\pi r^4} \{ [1 - 5(\hat{m} \cdot \hat{r})^2] \hat{r} + 2(\hat{m} \cdot \hat{r}) \hat{m} \}, \quad (4)$$

where  $\hat{r} \equiv \vec{r}/r$  and  $\hat{m} = (\cos(\omega_0 t)\hat{x} + \sin(\omega_0 t)\hat{y})$ . Note that as we are using one-particle Stokes' hydrodynamics, an excluded-volume force  $\vec{F}^{ev}$  must be included to keep particles from overlapping. This force is calculated from [21]

$$\vec{F}^{ev} = A \frac{3\mu_0 m^2}{4\pi(2a)^4} \hat{r} \exp \left[ -B \left( \frac{r}{2a} - 1 \right) \right], \quad (5)$$

where we assumed  $A = 2$  and  $B = 10$ . Similar repulsive forces have been used in previous works [21, 22]. The parameter  $A$  is chosen in order to give zero interaction force when the two particles aligned along the field direction and interacting with dipolar force, are in contact (i.e.  $r/2a = 1$ ). With  $B = 10$  the ratio between dipolar and excluded-volume forces of the two particles aligned with the field reaches the value ten (the value 0.1) when the distance between the particles increases to  $r/2a = 1.1$  (decreases to  $r/2a = 0.9$ ).

We rewrite the pair evolution equations in terms of the dimensionless distance between particle centres,  $R \equiv r/2a$ , and the angle of the pair orientation,  $\phi$ :

$$\frac{dR}{d\tau} = \frac{2}{R^4} [1 - 3 \cos^2(\omega_0 t_s \tau - \phi)] + 2A \exp[-B(R - 1)], \quad (6)$$

$$\frac{d\phi}{d\tau} = \frac{2}{R^5} \sin 2(\omega_0 t_s \tau - \phi), \quad (7)$$

where a timescale  $t_s \equiv 12^2 \eta / \mu_0 M^2$  which leads to a dimensionless time equal to  $\tau \equiv t/t_s$  has been introduced in equations (6) and (7). The temporal scale,  $t_s$ , gives a dimensionless rotating frequency equal to the Mason number  $\omega_0 t_s \equiv Ma$ , i.e. to the ratio of the viscous to magnetic forces. It means that the dynamics of the pair motion is governed by the Mason number. We rewrite equations (6) and (7) using the phase lag between the field and the pair orientation  $\alpha \equiv Ma\tau - \phi$

$$\frac{dR}{d\tau} = \frac{2}{R^4} [1 - 3 \cos^2 \alpha] + 2A \exp[-B(R - 1)], \quad (8)$$

$$\frac{d\alpha}{d\tau} = Ma - \frac{2}{R^5} \sin 2\alpha. \quad (9)$$

### 2.1. Dynamics at constant $Ma$

First, we study the problem using a constant  $Ma$ , i.e. the reported case in previous works [7, 8]. In agreement with

their results, we find two different regimes depending on the dimensionless driving frequency (or Mason number). Some examples are presented in figure 1(a), where the time evolution of the interparticle dimensionless distance  $R$ , after the transient, is plotted at various Mason numbers for the initial conditions  $R = 3$  and  $\alpha = 0$ . For low Mason numbers, a rigid doublet is formed, i.e. the interparticle distance remains constant at  $R = 1$  (see dotted line in figure 1(a)). This rigid doublet rotates uniformly and is phase-locked to the field. This rotation is governed by the equation  $\sin(2\alpha_0) = Ma/2$  (see equation (9)). For high Mason numbers, above a threshold value located at approximately 1.3, the pair goes through a periodic sequence of forward and backward rotations with additional radial oscillations (see dashed and solid lines in figure 1(a)). The amplitude of the radial oscillations decreases as  $Ma$  increases in agreement with the results found by Kashevsky and Novokova [8]. The angular dimensionless frequency of the radial oscillations,  $\omega_R$ , increases linearly when increasing the Mason number (see figure 1(b)).

We must point out that these results have been obtained considering the fluid resistance through the simple Stokes friction. However, it is well-known that once the pair approaches very close, smaller than the particle diameter, hydrodynamic particle–particle interaction occurs, and lubrication forces become important in order to describe the pair dynamics. Kashevsky and Kuzmin studied the dynamics of a system of two particles subject to a

rotating magnetic field taking into account the hydrodynamic interaction [10]. They found that the threshold frequency that separates the synchronous and asynchronous regimes shifts to a smaller value, i.e. the asynchronous rotation regime begins at lower Mason numbers. However, they did not find an appreciable change in the frequency of the radial oscillations when considering hydrodynamic interaction. The results we present in this work are based on the interplay between the modulation of the Mason number and the intrinsic radial oscillation of the system without modulation. Since these radial oscillations remain almost unaltered, it is expected that the same type of resonant-like phenomenon takes place when the hydrodynamic forces are accounted for.

### 3. Dynamics at modulated $Ma$

We have found in the previous section that the state of the system depends on the value of the Mason number. Therefore, it is expected that a time-dependent perturbation on  $Ma$  changes the state of the system. In this section we will analyse the pair dynamics when a perturbation on the Mason number is applied.

#### 3.1. Periodic perturbation

We have studied the effect of a periodic modulation on the Mason number, i.e.

$$Ma = Ma_0 + \Delta\Omega \sin(\Omega\tau), \quad (10)$$

where  $Ma_0$  is the average Mason number,  $\Delta\Omega$  is the amplitude of the modulation and  $\Omega$  is the modulation dimensionless frequency. We study the behaviour of the interparticle dimensionless distance  $R$  when a small modulation amplitude is applied ( $\Delta\Omega = 0.15$ ) at different modulation dimensionless frequencies (ranging from  $\Omega = 1$  to 5). Figure 2 shows the temporal evolution of the interparticle dimensionless distance and its corresponding power spectrum for different modulation frequencies at  $Ma_0 = 1.5$ . For  $\Omega = 1$  and  $\Omega = 3$ , a multiperiodic oscillation occurs in the interparticle distance (see figures 2(a), (b), (e), and (f)), being the two fundamental frequencies the respective frequency of the modulation  $\Omega$  and the corresponding frequency of the radial oscillations without modulation at  $Ma = 1.5$ ,  $\omega_R \simeq 1.8$  (see figure 1(b)). Combinations of both frequencies,  $\Omega \pm \omega_R$ , are also found. This result means that the well-known radial oscillation of the system without modulation still appears when the Mason number is periodically modulated. Therefore, two different movements govern the dynamics of the pair of magnetizable particles immersed in a non-magnetic fluid; the intrinsic radial oscillation, i.e. the natural oscillation of the system, and a periodic movement due to the external forcing on the Mason number. Now, a natural question arises, what will happen when the modulation frequency matches the natural frequency of the radial oscillations? The result is shown in figures 2(c) and (d). Now, only one peak and its harmonics appear, indicating that the frequency of the external forcing on  $Ma$  matches the intrinsic oscillation of the system, so a resonance phenomenon takes place.

To study how this resonance affects the behaviour of the average interparticle dimensionless distance,  $R_{\text{mean}}$ , we

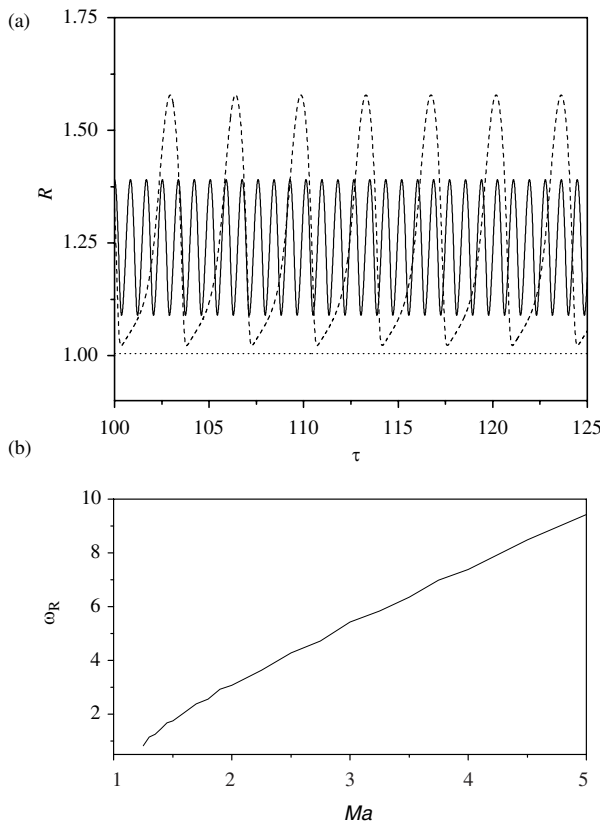


**Figure 1.** (a) Temporal evolution of the interparticle dimensionless distance  $R$ , after the transient, for the initial conditions  $R = 3$  and  $\alpha = 0$  at  $Ma = 0.5$  ( $\cdots$ ),  $Ma = 1.5$  ( $-\cdots-$ ), and  $Ma = 4$  ( $—$ ). (b) Angular dimensionless frequency of the radial oscillations  $\omega_R$  versus Mason number.

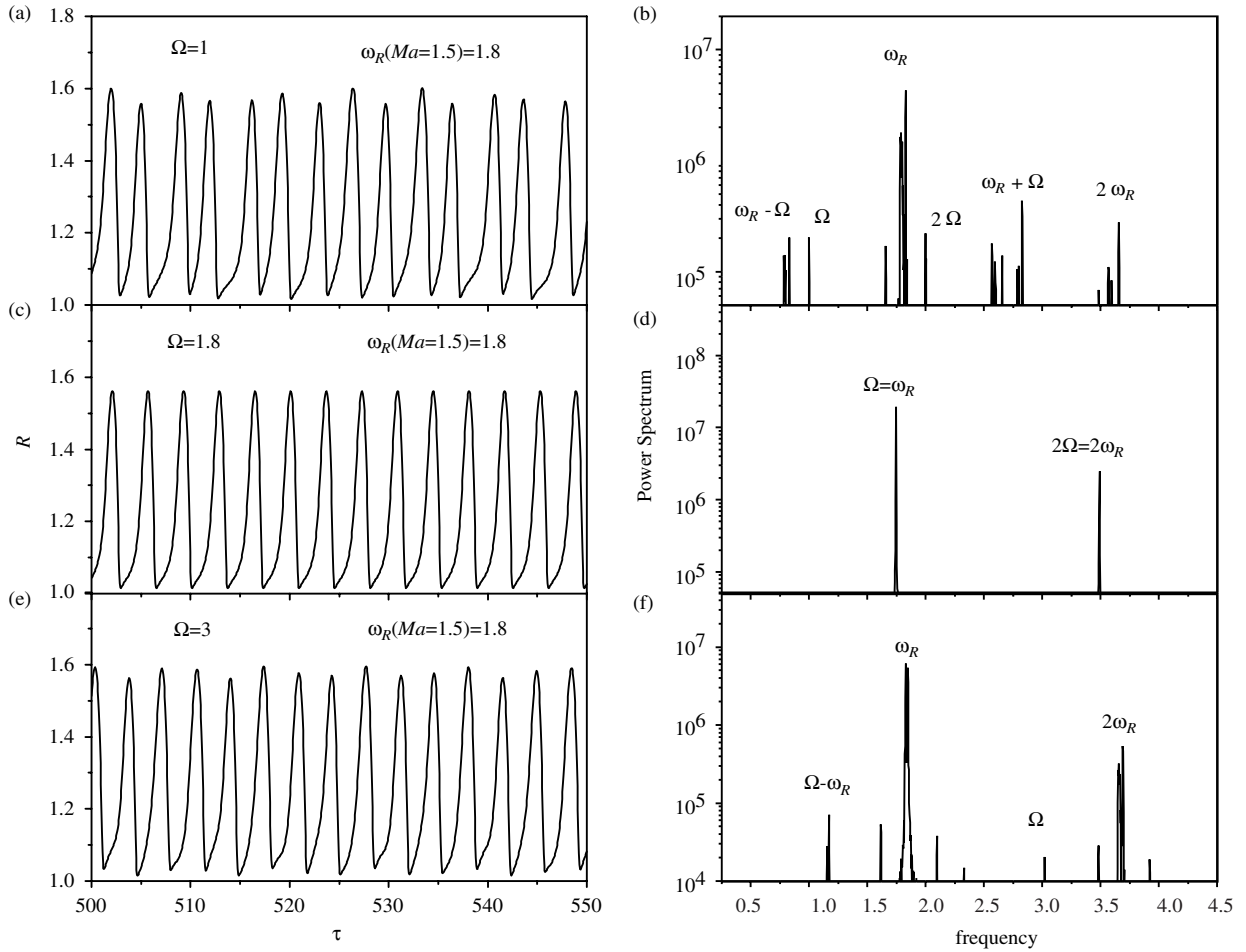


**Figure 2.** Temporal evolution of the interparticle dimensionless distance (plots (a), (c), and (e)) and its power spectrum (plots (b), (d), and (f)) for a modulation frequency  $\Omega = 1$  (plots (a) and (b)),  $\Omega = 1.8$  (plots (c) and (d)), and  $\Omega = 3$  (plots (e) and (f)). The parameters used are  $Ma_0 = 1.5$  and  $\Delta\Omega = 0.15$ .

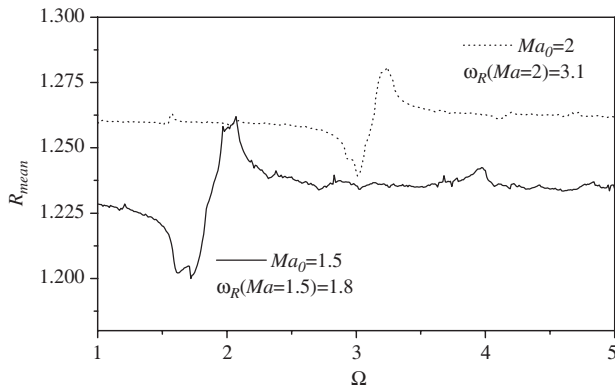


**Figure 3.** Average interparticle dimensionless distance  $R_{\text{mean}}$  versus modulation dimensionless frequency  $\Omega$  at two different average Mason numbers;  $Ma_0 = 1.5$  (—) and  $Ma_0 = 2$  (.....). The modulation amplitude is  $\Delta\Omega = 0.15$ .

have analysed  $R_{\text{mean}}$  when the Mason number is periodically modulated. The results of  $R_{\text{mean}}$  versus the modulation dimensionless frequency  $\Omega$  are shown in figure 3 for a small modulation amplitude  $\Delta\Omega = 0.15$ , at two different average Mason numbers. In both cases,  $R_{\text{mean}}$  is nearly constant and close to the value without modulation through most of the

range of modulation frequencies. However, when  $\Omega$  comes close to the intrinsic radial oscillation frequency associated with its average Mason number  $\omega_R(Ma_0)$ ,  $R_{\text{mean}}$  changes noticeably. The curve has a sharp minimum at a value of  $\Omega$  which is slightly smaller than  $\omega_R$ , and a sharp maximum at a value slightly greater than  $\omega_R$ . Between the minimum and the maximum, the function increases with increase in the modulation frequency. This resonant curve ( $\Omega$ ,  $R_{\text{mean}}$ ) is similar to the well-known dispersion curve which explains the variation of the real part of the refractive index of a medium with the electromagnetic field frequency [23]. As we mention above, the intrinsic radial oscillation frequency  $\omega_R$  is a function of the Mason number (see figure 1(b)). Therefore, when we modulate the  $Ma$ , the natural frequency of the pair system without modulation  $\omega_R$  gets broader around its value so there is a range of modulation frequencies  $\Omega$  that resonate. The distance between the minimum and maximum peaks roughly measures the spectral width of the intrinsic oscillation. Then, this spectral width should depend on the modulation amplitude value since more frequencies are incorporated into the intrinsic radial oscillation as  $\Delta\Omega$  increases. In figure 3, both curves have the same modulation amplitude, so the distance between the minimum and maximum peaks is approximately the same for both curves, in agreement with our hypothesis. To study the

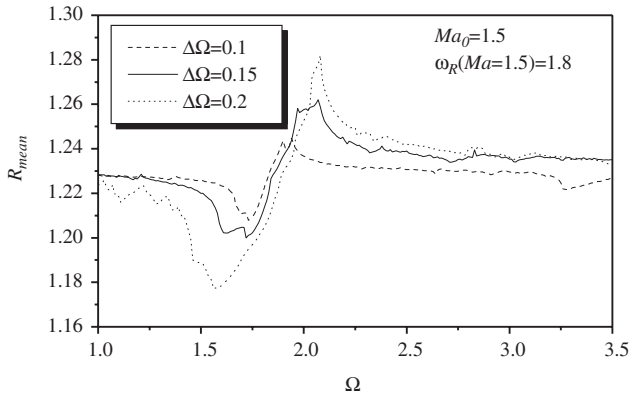


**Figure 4.** Average interparticle dimensionless distance  $R_{\text{mean}}$  versus modulation dimensionless frequency  $\Omega$  at different modulation amplitudes;  $\Delta\Omega = 0.1$  (---),  $\Delta\Omega = 0.15$  (—), and  $\Delta\Omega = 0.2$  (·····). The average Mason number is  $Ma_0 = 1.5$ .

dependence of the distance on the modulation amplitude, the average distance  $R_{\text{mean}}$  versus  $\Omega$  at  $Ma_0 = 1.5$  for different modulation amplitudes is plotted in figure 4. It can be seen in this figure how the spectral width, i.e. the distance between the minimum and maximum peaks, increases as the modulation amplitude increases. We also observe that the change in the value of  $R_{\text{mean}}$  is larger as the modulation amplitude increases.

From the previous results it is clear that a type of resonant phenomenon is taking place in the system, since two periodic oscillations coexist. Moreover, we have seen that the average interparticle distance can be controlled, by means of the periodic modulation, for modulation frequencies close to the intrinsic radial oscillation frequency that appears in the system without modulation.

### 3.2. Random perturbation

In this section we introduce fluctuations in the Mason number by means of a zero-mean, Gaussian white noise,  $g(\tau)$ , with autocorrelation function

$$\langle g(\tau)g(\tau') \rangle = 2D\delta(\tau - \tau'), \quad (11)$$

and intensity  $D$ . Under these conditions the Mason number can be read as

$$Ma = Ma_0 + g(\tau). \quad (12)$$

We study the behaviour of the average interparticle dimensionless distance  $R_{\text{mean}}$  when a noise source is applied to the Mason number. Figure 5 shows  $R_{\text{mean}}$  versus noise strength  $D$  at  $Ma_0 = 1.5$ . Here,  $R_{\text{mean}}$  has been averaged over 500 realizations. We can see in this figure that there is a value of the noise strength at which the average interparticle dimensionless distance reaches a minimum. This optimum noise strength gives a value of  $R_{\text{mean}}$  slightly lower than the value obtained without the random source, although the variation is not appreciable.

Now we consider the combined effect of modulating the Mason number with a periodic modulation and a noise source to study the phenomenon of SR. Thus, we introduce a weak periodic modulation, as in equation (10), and a noise source, as

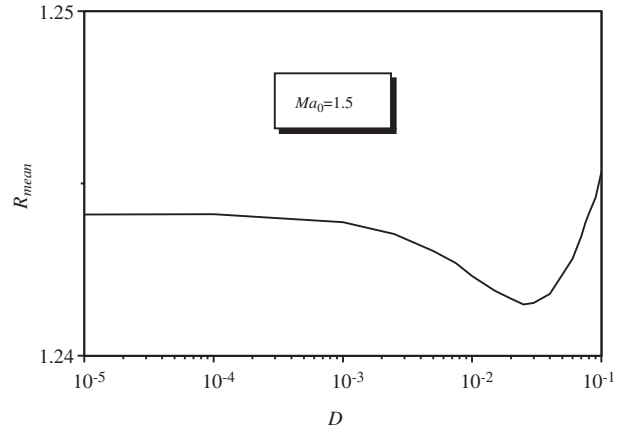


**Figure 5.** Average interparticle dimensionless distance  $R_{\text{mean}}$  versus the noise strength  $D$  at  $Ma_0 = 1.5$ .

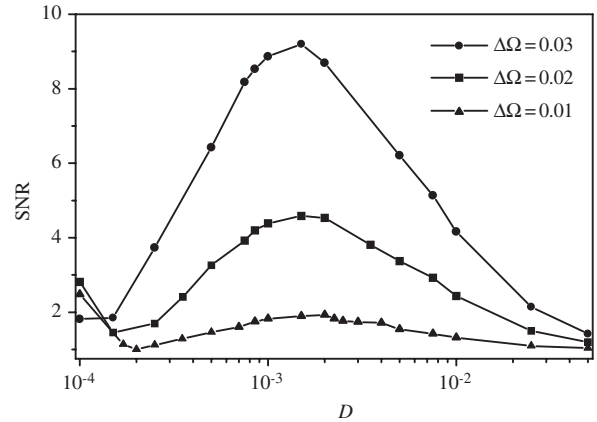


**Figure 6.** SNR as a function of the input noise power for a modulation amplitude  $\Delta\Omega = 0.03$  (●),  $\Delta\Omega = 0.02$  (■), and  $\Delta\Omega = 0.01$  (▲). The parameters used are  $Ma_0 = 1.2$  and  $\Omega = 0.8$ .

in equation (12) on the Mason number. Therefore, the Mason number can be read as

$$Ma = Ma_0 + \Delta\Omega \sin(\Omega\tau) + g(\tau), \quad (13)$$

where all the parameters have been defined above. In order to get the rigid doublet state ( $R = 1$ ) in the absence of noise we take an average Mason number  $Ma_0 = 1.2$  (slightly smaller than the threshold value), and we choose a small value of the modulation amplitude ( $\Delta\Omega < 0.05$ ) to avoid reaching the threshold Mason number placed around 1.3.

To observe SR, we numerically integrate equations (8), (9), and (13). We calculate the power spectrum of the temporal evolution of the interparticle dimensionless distance  $R$ . In particular, for each set of parameters ( $\Delta\Omega$ ,  $\Omega$ ,  $D$ ), we calculate an averaged power spectrum over 500 realizations. These spectra show a principal peak above the noise background located at the modulation frequency ( $\Omega$ ), which indicates the existence of a coherent movement. To analyse the dependence of the noise-induced coherent motion on the noise strength, we calculate the ratio of the peak of the signal and the broadband noise level at the signal frequency, which is the signal-to-noise ratio (SNR). Figure 6 shows the SNR versus  $D$  for a modulation frequency  $\Omega = 0.8$ . We observe a maximum in the SNR for the

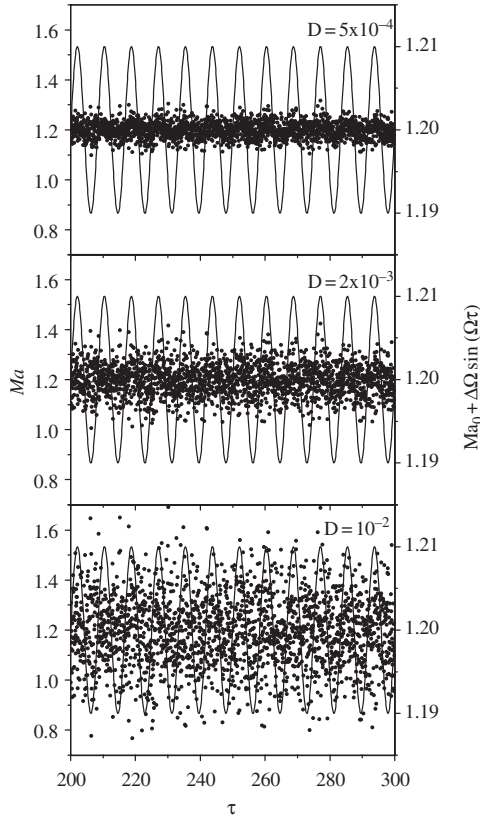


**Figure 7.** On the left axis we plot the Mason number (points), given by equation (13), versus time for an individual realization using different noise strengths. On the right axis we also plot the periodically modulated Mason number, i.e.  $Ma_0 + \Delta\Omega \sin(\Omega\tau)$  (—). The parameters used are  $Ma_0 = 1.2$ ,  $\Delta\Omega = 0.01$ , and  $\Omega = 0.8$ .

three curves corresponding to different modulation amplitudes, which indicates the presence of SR.

To understand how SR takes place in our system, we analyse in more detail the dynamics for the particular case  $\Delta\Omega = 0.01$ . In this case, the value of the noise strength that gives a maximum SNR is  $D \equiv D_r \simeq 2 \times 10^{-3}$  (see figure 6). Figure 7 shows the temporal evolution of the Mason number (points), given by equation (13), for an individual realization using different noise strengths. For comparison, we also plot the periodically modulated Mason number  $Ma_0 + \Delta\Omega \sin(\Omega\tau)$  on the right axis (solid line). For  $D < D_r$ , the Mason number does not reach the threshold value, so the two particles remain in the rigid doublet state, i.e.  $R \simeq 1$ . However, at  $D \simeq D_r$ , the noise source causes  $Ma$  to surpass the threshold value allowing radial oscillation cycles in the pair dynamics. We can see in figure 7 (centre graph) that  $Ma$  roughly surpasses the threshold value once every period. We define an average dimensionless time between threshold crossing induced by the noise as  $T_N(D)$ , which is a function of the noise strength. A statistical synchronization takes place when this time  $T_N$  is comparable with the period  $2\pi/\Omega$  of the modulation signal. This yields the timescale matching condition for SR, i.e.

$$T_N(D_r) = \frac{2\pi}{\Omega}. \quad (14)$$

For higher noise levels ( $D > D_r$ ),  $Ma$  crosses the threshold many times but no correlation between the average time

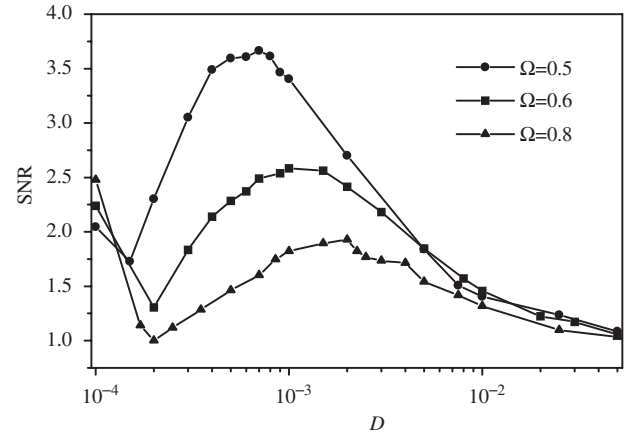


**Figure 8.** SNR as a function of the input noise power for a dimensionless modulation frequency  $\Omega = 0.5$  (●),  $\Omega = 0.6$  (■), and  $\Omega = 0.8$  (▲). The parameters used are  $Ma_0 = 1.2$  and  $\Delta\Omega = 0.01$ .

between threshold crossing and the modulation signal period is observed.

Equation (14) implies that  $D_r$  depends on the modulation frequency  $\Omega$ . To verify this dependence, the SNR at  $\Delta\Omega = 0.01$  for different modulation frequencies is plotted in figure 8. We see in this figure that the maximum of the SNR shifts to larger  $D$  values as the frequency increases.

#### 4. Conclusions

We have theoretically studied the temporal dynamics on simple MR suspensions under rotating magnetic fields. We consider a system that consists of a pair of magnetizable particles suspended in a non-magnetic fluid subject to a rotating magnetic field. In such a system there are two different dynamic regimes depending on the Mason number. At low Mason numbers a rigid doublet rotates phase-locked to the field, while at higher Mason numbers an asynchronous rotation of the pair with additional radial oscillations appears.

The dynamics of this system when a modulation on the Mason number is applied has been studied. Using a periodic modulation, we observed that a resonant-like phenomenon between the periodic modulation of  $Ma$  and the intrinsic radial oscillation of the system without modulation occurs. The average interparticle distance versus the modulation frequency curve shows the typical behaviour of the dispersion curve of a medium [23]. The curve has a sharp minimum at a value of the modulation frequency which is slightly smaller than the intrinsic radial oscillation frequency, and a sharp maximum at a value slightly greater than the intrinsic radial oscillation frequency. For a random perturbation on the Mason number we obtained an optimum noise strength at which the average interparticle distance reaches a minimum, this value being lower than the value without the perturbation.

We also presented evidence of SR in MR suspensions under rotating magnetic fields when a weak periodic modulation and a noise source are added to the Mason number. We have analysed the SNR versus noise power for different frequencies and amplitudes of the modulation, and in all cases a maximum in the SNR has been found. This indicates the

presence of SR. The behaviour of the system can be explained by a crossing at the Mason number threshold.

### Acknowledgments

This work was partially supported by the Projects No BFM2000-0796 and No BFM2000-0019 (Spain).

### References

- [1] Larson R G 1999 *The Structure and Rheology of Complex Fluids* (New York: Oxford University Press)
- [2] Lemaire E, Grasselli Y and Bossis G 1992 *J. Phys. II* (France) **2** 359
- [3] Hwang Y H and Wu X I 1994 *Phys. Rev. E* **49** 3102
- [4] Wirtz D and Fermigier M 1994 *Phys. Rev. Lett.* **72** 2294
- [5] Promislow J H E, Gast A P and Fermigier M 1995 *J. Chem. Phys.* **102** 5492
- [6] Melle S, Rubio M A and Fuller G G 2001 *Phys. Rev. Lett.* **87** 115501
- [7] Helgesen G, Pieranski P and Skjeltorp A T 1990 *Phys. Rev. Lett.* **64** 1425  
Helgesen G, Pieranski P and Skjeltorp A T 1990 *Phys. Rev. A* **42** 7271
- [8] Kashevsky B E and Novokova A L 1989 *Magnetohydrodynamics* **25** 304
- [9] Kashevsky B E 1990 *J. Magn. Magn. Mater.* **85** 57
- [10] Kashevsky B E and Kuzmin V A 1996 *J. Phys. D: Appl. Phys.* **29** 2579
- [11] Meakin P and Skjeltorp A T 1993 *Appl. Phys.* **42** 1
- [12] Melle S, Fuller G G and Rubio M A 2000 *Phys. Rev. E* **61** 4111
- [13] Melle S, Calderón O G, Fuller G G and Rubio M A 2002 *J. Coll. Inter. Sci.* **247** 200
- [14] Melle S, Calderón O G, Fuller G G and Rubio M A 2002 *J. Non-Newtonian Fluid Mech.* **102** 135
- [15] Gast A P and Zukoski C F 1989 *Adv. Coll. Inter. Sci.* **30** 153
- [16] Volkova O, Cutillas S and Bossis G 1999 *Phys. Rev. Lett.* **82** 233
- [17] Martin J E 2001 *Phys. Rev. E* **63** 011406
- [18] Gammaitoni L, Hanggi P, Jung P and Marchesoni F 1998 *Rev. Mod. Phys.* **70** 223  
Wiesenfeld K and Jaramillo F 1998 *Chaos* **8** 539
- [19] Pérez-Madrid A K and Rubí J M 1995 *Phys. Rev. E* **51** 4159
- [20] Alarcón T and Pérez-Madrid A K 2001 *Phys. Rev. E* **63** 041112
- [21] Mohebi M, Jamasbi N and Liu J 1996 *Phys. Rev. E* **54** 5407
- [22] Klingenberg D J, Swol F van and Zukovski C F 1989 *J. Chem. Phys.* **91** 7888
- [23] Born M and Wolf E 1980 *Principles of Optics* (Oxford: Pergamon) p 93